Inferring Physiological Properties of Motor Neurons using Neural Posterior Estimation

Pranav Mamidanna [1 2] **Dario Farina** [2]

Abstract

Measuring or inferring the physiological properties of motor neurons, such as during disease progression or aging, remains challenging, often requiring longitudinal invasive measurements or analysis techniques based on simplifying assumptions. Here we use the framework of simulation-based inference to train neural density estimators that directly infer the posterior distribution of properties of interest (i.e., the physiological properties most likely to explain the observations) by simulating from a state-of-the-art electromyography simulator. We not only surpass conventional methods in accuracy and sensitivity, but also infer properties that have so far been impossible to measure. We believe this will significantly impact the possibilities for both clinical and research contexts in motor neurophysiology.

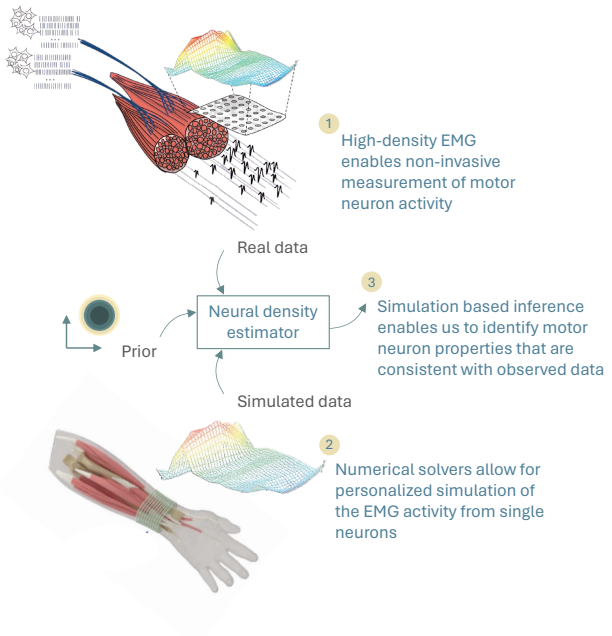

Figure 1. Inferring physiological properties of MNs. (Elements of the figure have been modified from Maksymenko et al. 2023, and Farina & Holobar 2015 with due permissions.)

1. Introduction

Motor neurons (MN) are fundamental components of the motor system, translating our intention to move into actual movement. Originating in the spinal cord, these neurons innervate muscle fibers, collectively activating them to produce movement. Estimating the physiological properties of MNs, such as the number of muscle fibers they innervate and the conduction velocity of these fibers, provides critical insights into the mechanisms by which the brain controls movement in health and disease. This understanding is particularly vital as alterations in MN properties can serve as biomarkers for various conditions, including neuromotor disorders like amyotrophic lateral sclerosis (ALS) and healthy ageing. Identifying and monitoring these alterations not only sheds light on the underlying mechanisms of these conditions but also holds promise for evaluating the efficacy of treatments and interventions.

Despite the importance of understanding MN properties, accurately measuring them remains challenging. Current methods often rely on invasive procedures, which are uncomfortable and impractical for routine use, while yet other properties cannot be feasibly measured in vivo (Mills & Shaw, 2020). Surface electromyography (sEMG) offers a promising noninvasive alternative by recording the electrical activity of MNs through electrodes placed on the skin. These surface action potentials (SAPs, the 'electrical signatures' of individual MNs) provide valuable insights into their physiology. However, traditional methods of analyzing these SAPs to infer properties of interest are based on simplifying assumptions, limiting their accuracy and applicability.

To overcome these limitations, we propose using advanced

[*]Equal contribution [1]Imperial-X Center for AI in Science, Imperial College London, United Kingdom [2]Department of Bioengineering, Imperial College London, United Kingdom. Correspondence to: Pranav Mamidanna <pm1222@ic.ac.uk>.

Accepted by the Structured Probabilistic Inference & Generative Modeling workshop of ICML 2024, Vienna, Austria.

modeling techniques and modern machine learning (Figure 1). The generation and propagation of electrical activity in muscles – from their origin in the muscle belly through biological tissues to the skin – is well understood. Sophisticated forward simulators have been developed to model this process accurately at a personalized scale (Maksymenko et al., 2023; Ma et al., 2022). Recent advances in simulation-based inference (SBI), particularly techniques that leverage the expressivity of neural density estimators, have transformed the ability to draw inferences from implicit models defined by such complex simulators (Cranmer, 2020). Neural posterior estimation (Papamakarios & Murray, 2016; Lueckmann et al., 2017; Greenberg et al., 2019), for instance, trains a conditional density estimator $q(\theta|x)$, given access only to a simulator that can generate $x \sim p(x|\theta)$. As a result, such SBI techniques readily represent uncertainty in multi-dimensional settings and handle inverse problems naturally. Subsequently, these methods have shown success in various fields, including astrophysics (Dax et al., 2021; 2023), neuroscience (Gonçalves et al., 2020; Boelts et al., 2022), and more recently cardivascular electrophysiology (Wehenkel et al., 2023; Senouf et al., 2023).

In this paper, we leverage state-of-the-art EMG simulators and apply simulation-based inference techniques to improve the estimation of MN properties. By comparing our results with traditional methods, we demonstrate significant improvements in the accuracy and reliability of these inferences. Our approach offers a substantial advancement in the noninvasive assessment of MN physiology, with broad applications in both clinical and research contexts.

2. Simulating the electrical activity of motor neurons

Biophysical models of MN SAPs proceed by first modelling the propagation of an action potential across the muscle fibres, and the subsequent 'volume conduction' effects experienced by the generated electric field as it passes through surrounding biological tissues and reaches the electrodes located on the skin (Merletti & Farina, 2016). The former is modelled as a travelling dipole, where the potential and current density source in the muscle fibre are given by

$$\begin{aligned} V_m(z) &= 96z^3e^{-z} - 90 \\ I(z,t) &= f(\frac{d^2V_m}{dt^2}, \gamma, z_i, \nu, \ell) \end{aligned} \tag{1}$$

where V_m is the membrane potential, I is the current density source, z is the location along the muscle fibre whose 3-D path is γ and length is ℓ, ν is the propagation (or conduction) velocity and z_i is the location of the neuromuscular junction – where the motor neuron innervates the muscle fibres.

The effect of the volume conductor is then modelled using the quasi-static Maxwell's equations with Neumann boundary conditions as

$$\begin{aligned} \nabla \cdot (\sigma \nabla \phi) &= -I \quad \text{in } \Omega, \\ \sigma \frac{\partial \phi}{\partial \boldsymbol{n}} &= \sigma \nabla \phi \cdot \boldsymbol{n} = 0 \quad \text{on } \partial\Omega, \end{aligned} \tag{2}$$

where $\Omega \subset \mathbb{R}^3$ is the domain of the volume conductor, $\sigma(z)$ denotes the conductivity tensor at each point in Ω, $\phi(z)$ is the electric potential, and $\boldsymbol{n}$ is the outward pointing surface normal to $\partial\Omega$. These equations can be solved numerically using finite element solvers for arbitrarily complex volume conductor geometries. Recent innovations (Maksymenko et al., 2023) also make it feasible to create personalized simulation models specific to an individual's anatomy, captured using magnetic resonance images (MRIs).

However, these simulators are still computationally expensive, especially for workloads often required in SBI. To overcome this limitation, Ma et al. 2022 built a conditional generative model, trained to mimic the numerical model mentioned before, that outputs the SAP given 4 important physiological parameters, including 3-D location of the MN z_i, conduction velocity ν, fibre density or the number of fibres innervated by the muscle ρ, and the average length of the innervated fibres $\bar{\ell}$. Specifically, they build a model capable of simulating SAPs from 8 superficial muscles of the forearm captured with a grid of 10×32 electrodes placed around the distal third of an individual's right forearm (see 1). The SAPs are modelled to be approximately 48ms in duration, corresponding to 96 samples at 2048 Hz. Notably, the emulator uses a normalized range between 0.5 and 1 for each dimension of the parameter vector. For the rest of this paper, we limit our attention to this 'emulator' of SAPs.

3. Experiments

In essence, we have access to a high-fidelity emulator $g : \Theta \to \mathcal{X}$, that given a 6-D vector of parameters $\theta \in \Theta$, (i.e., 3-D location z_i, ν, ρ, and ℓ), returns a simulated SAP $\boldsymbol{x} \in \mathcal{X}$. Our objective is to solve the corresponding inverse problem of mapping SAPs to plausible parameters.

In this work, we consider a dataset of 1000 distinct SAPs generated by uniformly sampling Θ across the 6-D space using a latin-hypercube sampling strategy. We apply the following methods to solve the inverse problem, and report the accuracy and sensitivity of each method.

3.1. Simulation-based inference

We considered two SBI approaches in this paper. Given that in a typical experimental EMG recording session, SAPs of the order of ten to hundred motor neurons can be recorded, we trained an amortized neural posterior estimation (NPE) algorithm. Specifically, we trained a masked autoregressive

flow network with 5 flow transforms, each with two blocks of 50 hidden units, tanh activation and batch normalization, using a simulation budget of 100,000 samples. A uniform prior over the support of the parameters was used here, but knowledge of experimental recording such as the spatial location of the muscle under investigation or its maximum length can be used to devise more informative priors.

Given the high dimensionality of the input SAPs ($10 \times 32 \times 96$), we used an embedding network to jointly learn summarizing features of the data. Here, we used a simple 3-D convolutional network, mimicking the feature extractor of the emulator (Ma et al., 2022). We used 3 convolutional layers with (64, 32, and 16) 3-D convolutional kernels of size 3, and stride 2, with a ReLU activation. The resulting output was passed through a single linear layer to generate a 64-dimensional output, which was used by the NPE algorithm.

Further, as a baseline, we performed classical approximate bayesian computation (ABC) using the sequential monte-carlo ABC (SMCABC) algorithm. While this is not an amortized algorithm, we used a simulation budget of 100,000 samples here too, given that sampling from the emulator was cheap, and since lower simulation budgets were too restrictive to narrow the search space for SMCABC. We used euclidean distance in data space as the distance measure. We used an initial population of 5000, with a population size of 1000 for the reminder of the algorithm. The perturbation kernel, which controls the exploration of the parameter space, was set to scale by 0.5 with respect to the empirical covariance from the previous population, while the quantile-based acceptance tolerance's decay was set to 0.2. For further information about the algorithm see Lueckmann et al. 2021.

All experiments were conducted using the `sbi` package (Tejero-Cantero et al., 2020) and the code to reproduce the experiments will be made open access upon acceptance.

3.2. Conventional methods

We compared the performance of the NPE and SMCABC algorithms against conventional methods used to determine MN location and conduction velocity. It is important to note that there are no existing methods that can directly estimate the fibre density or the fibre length from SAPs.

The state-of-the-art method for estimating the 3-D location of MNs, by Lundsberg et al. 2024, proceeds by first estimating the x-y location on the electrode grid with the highest signal intensity. This is done by fitting a 2-D gaussian kernel to the peak-to-peak amplitudes of the SAPs. Then, they use a simplified cylindrical volume conductor to model signal attenuation properties of the peak-to-peak SAP, and reverse engineer the distance of the source from the electrodes given the observed attenuation from the maximally

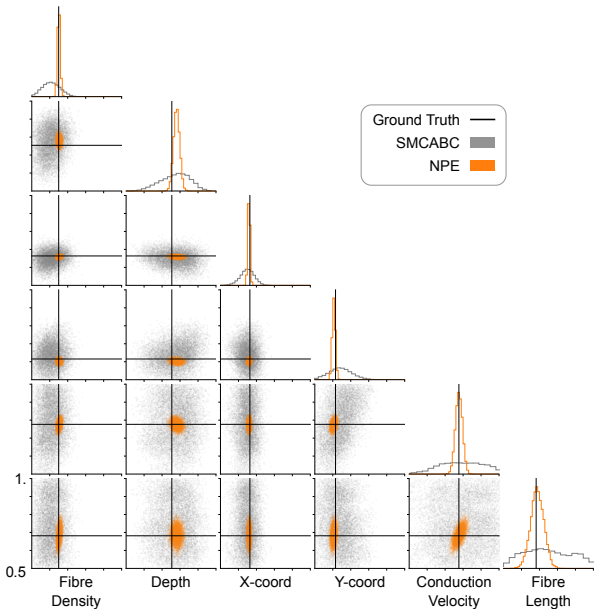

Figure 2. Inferred posteriors for the 6-D parameter vector by NPE (orange) and SMCABC (gray) for a sample observation (ground truth values shown in black). Univariate and pairwise marginals are plotted by using 10,000 samples drawn from the posteriors. Interestingly, even with identical simulation budgets, NPE far outperforms SMCABC despite the amortization.

active electrode outwards. Importantly, this method requires that the MN be located within the space covered by the electrode grid. On the contrary, the inverse modelling approach doesn't have such a restriction as long as the SAP of such a MN can be simulated, and creates a non-zero potential on the electrodes.

To estimate conduction velocity, we use an algorithm that estimates the delay between the signal from successive electrodes along the fiber direction (Farina et al., 2001; Casolo et al., 2023). However, the algorithm assumes that the electrodes grids are aligned with the muscle fibre paths γ. Moreover, it has been shown to be sensitive to initial conditions.

3.3. Metrics

As indicated before, we report results on the 1000 ground truth parameters sampled uniformly from Θ. Since both SBI approaches both recover parameters in Θ-space directly, we report mean relative error across the ground truth parameters to report their accuracy. On the other hand, the conventional methods estimate the location and velocity parameters in 'true units', given the inter-electrode distances, and the sampling frequency. We convert these back into the normalized range of the emulator using the mapping from the original

Method →	NPE	SMCABC	Conventional
Property			
z_i	**0.02 ± 0.01**	0.17 ± 0.11	0.07 ± 0.09
ρ	**0.009 ± 0.01**	0.18 ± 0.12	-
ν	**0.02 ± 0.01**	0.14 ± 0.11	0.04 ± 0.06
ℓ	**0.03 ± 0.02**	0.18 ± 0.08	-

Table 1. Accuracy (mean relative error ± standard deviation across the 1000 ground truth samples) of SBI and conventional approaches to estimating MN properties. Bold indicates the method with best performance.

publication (Ma et al., 2022), and similarly report mean relative errors in this normalized range, for consistency. In Table 1, results are displayed for the 3-D location directly, instead of each of the coordinates separately.

Additionally, we generated a probability-probability plot for the NPE posteriors by first evaluating the percentile score of each ground truth parameter value within its inferred marginal posterior. We then sorted the percentile scores and generated the empirical cumulative distribution function (CDF) to compare to the theoretical Uniform CDF.

4. Results

Figure 2 shows the resulting posterior distributions from both NPE and SMCABC. The NPE estimated posteriors were noticeably narrower than their SMCABC counterparts, despite the amortization in NPE and a simulation budget of only 10^5 samples. Highest uncertainty was seen in the fibre length parameter, arguably the hardest parameter to infer since the electrodes in the emulator do not cover the entire muscle belly of any of the 8 modelled muscles.

Full results in Table 1 corroborate the impressions of the density plots from Figure 2. Mean relative error for NPE was at most 5-6% of the normalized range (i.e., the mean relative error of 0.03 in ℓ corresponds to 6% given the range is 0.5), which is almost one order of magnitude more accurate than the SMCABC, while also far outperforming established methods in the field. Particularly, the variability of the relative errors for NPE with respect to the conventional methods was much lower. Importantly, NPE enables us to infer properties such as fibre density and average fibre length of the innervated fibres, that have never before been directly estimated using SAPs. Impressively, on these parameters, NPE only had a mean relative error of 2% and 6% for fibre density and fibre length respectively.

Additionally in Figure 3, we present the P-P plot of the NPE posteriors for the ground truth test data. This plot presents the CDF of the percentile score of the true parameter value within its inferred marginal posterior. For true posteriors, the percentiles are uniformly distributed, so the CDF is a diagonal. Overall, we found that the CDFs for NPE lie close to the diagonal for each of the parameters, indicating a strong agreement with true posteriors.

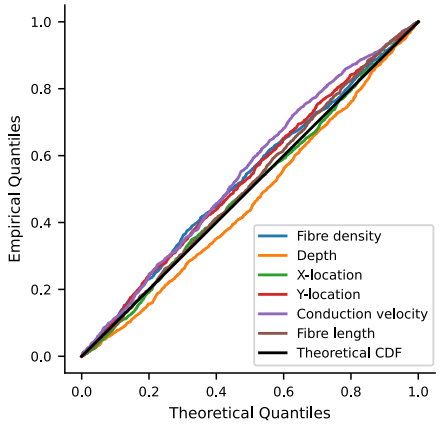

Figure 3. Probability-probability plot of the NPE posteriors for the ground truth test data.

5. Discussion

In this paper, we have demonstrated the success of Neural Posterior Estimation (NPE) on an important problem in motor neurophysiology: identifying the physiological properties of motor neurons. We used NPE together with a high-fidelity simulator of EMG signals to achieve this goal. We tested its performance against an SMCABC algorithm and conventional methods used in the field. While NPE outperforms all tested methods, it crucially also enables the estimation of properties that are currently unestimable by other methods.

A limitation of our current efforts is that we only tested the methods on data that is entirely consistent with the training distribution, i.e., all data was synthetically generated through the emulator. Therefore, we still lack experimental evidence for the success of these methods. Moving forward, we need methods that take into consideration the effects of model misspecification inherent in current biophysical models, however accurate they may be. The sim-to-real gap is a major challenge to the success of these methods, and therefore needs careful handling of all sources of uncertainties involved. It is also of interest to consider a hierarchical inference framework, since properties such as those pertaining to muscle architecture and tissue conductivity are shared among sets of motor neurons, and including such relationships in the inference pipeline can facilitate estimation of such shared properties. We believe that sophisticated simulators and sbi approaches are poised to revolutionize the field of motor neurophysiology.

References

Boelts, J., Lueckmann, J.-M., Gao, R., and Macke, J. H. Flexible and efficient simulation-based inference for models of decision-making. *Elife*, 11:e77220, 2022.

Casolo, A., Maeo, S., Balshaw, T. G., Lanza, M. B., Martin, N. R., Nuccio, S., Moro, T., Paoli, A., Felici, F., Maffulli, N., et al. Non-invasive estimation of muscle fibre size from high-density electromyography. *The Journal of Physiology*, 601(10):1831–1850, 2023.

Cranmer, K. The frontier of simulation-based inference. *Proceedings of the National Academy of Sciences*, 2020. doi: 10.1073/pnas.1912789117. URL https://www.pnas.org/doi/10.1073/pnas.1912789117.

Dax, M., Green, S. R., Gair, J., Macke, J. H., Buonanno, A., and Schölkopf, B. Real-time gravitational wave science with neural posterior estimation. *Physical review letters*, 127(24):241103, 2021.

Dax, M., Green, S. R., Gair, J., Pürrer, M., Wildberger, J., Macke, J. H., Buonanno, A., and Schölkopf, B. Neural importance sampling for rapid and reliable gravitational-wave inference. *Physical Review Letters*, 130(17):171403, 2023.

Farina, D. and Holobar, A. Human machine interfacing by decoding the surface electromyogram [life sciences]. *IEEE Signal Processing Magazine*, 32(1):115–120, 2015. doi: 10.1109/MSP.2014.2359242.

Farina, D., Muhammad, W., Fortunato, E., Meste, O., Merletti, R., and Rix, H. Estimation of single motor unit conduction velocity from surface electromyogram signals detected with linear electrode arrays. *Medical and Biological Engineering and Computing*, 39:225–236, 2001.

Gonçalves, P. J., Lueckmann, J.-M., Deistler, M., Nonnenmacher, M., Öcal, K., Bassetto, G., Chintaluri, C., Podlaski, W. F., Haddad, S. A., Vogels, T. P., et al. Training deep neural density estimators to identify mechanistic models of neural dynamics. *Elife*, 9:e56261, 2020.

Greenberg, D., Nonnenmacher, M., and Macke, J. Automatic posterior transformation for likelihood-free inference. In *International Conference on Machine Learning*, pp. 2404–2414. PMLR, 2019.

Lueckmann, J.-M., Goncalves, P. J., Bassetto, G., Öcal, K., Nonnenmacher, M., and Macke, J. H. Flexible statistical inference for mechanistic models of neural dynamics. *Advances in neural information processing systems*, 30, 2017.

Lueckmann, J.-M., Boelts, J., Greenberg, D. S., Gonçalves, P. J., and Macke, J. H. Benchmarking simulation-based inference, 2021.

Lundsberg, J., Björkman, A., Malesevic, N., and Antfolk, C. Inferring position of motor units from high-density surface emg. *Scientific Reports*, 14(1):3858, 2024.

Ma, S., Clarke, A. K., Maksymenko, K., Deslauriers-Gauthier, S., Sheng, X., Zhu, X., and Farina, D. Conditional generative models for simulation of emg during naturalistic movements. *arXiv preprint arXiv:2211.01856*, 2022.

Maksymenko, K., Clarke, A. K., Mendez Guerra, I., Deslauriers-Gauthier, S., and Farina, D. A myoelectric digital twin for fast and realistic modelling in deep learning. *Nature Communications*, 14(1):1600, 2023.

Merletti, R. and Farina, D. *Surface electromyography: physiology, engineering, and applications*. John Wiley & Sons, 2016.

Mills, K. and Shaw, C. The evolving role of surface electromyography in amyotrophic lateral sclerosis: A systematic review. *Clinical Neurophysiology*, 131(4):942–950, 2020.

Papamakarios, G. and Murray, I. Fast ε-free inference of simulation models with bayesian conditional density estimation. *Advances in neural information processing systems*, 29, 2016.

Senouf, O., Behrmann, J., Jacobsen, J.-H., Frossard, P., Abbe, E., and Wehenkel, A. Inferring cardiovascular biomarkers with hybrid model learning. In *NeurIPS 2023 Workshop on Deep Learning and Inverse Problems*, 2023.

Tejero-Cantero, A., Boelts, J., Deistler, M., Lueckmann, J.-M., Durkan, C., Gonçalves, P. J., Greenberg, D. S., and Macke, J. H. sbi: A toolkit for simulation-based inference. *Journal of Open Source Software*, 5(52):2505, 2020. doi: 10.21105/joss.02505. URL https://doi.org/10.21105/joss.02505.

Wehenkel, A., Behrmann, J., Miller, A. C., Sapiro, G., Sener, O., Cuturi, M., and Jacobsen, J.-H. Simulation-based inference for cardiovascular models. *arXiv preprint arXiv:2307.13918*, 2023.